CALIFORNIA PATH PROGRAM
INSTITUTE OF TRANSPORTATION STUDIES
UNIVERSITY OF CALIFORNIA, BERKELEY

Adaptive Throttle Control for Speed Tracking

Z. Xu
P. Ioannou

University of Southern California

California PATH Research Paper

UCB-ITS-PRR-94-09

This work was performed as part of the California PATH Program of the University of California, in cooperation with the State of California Business, Transportation, and Housing Agency, Department of Transportation.

April 1994

ISSN 1055-1425

Adaptive Throttle Control for Speed Tracking*

Z. Xu and P. Ioannou
Southern California Center
for Advanced Transportation Technologies
EE - Systems, EEB 200B
University of Southern California
Los Angeles, CA 90089-2562

Abstract. Electronic throttle control is an important part of every advanced vehicle control system. In this paper we design an adaptive control scheme for electronic throttle that achieves good tracking of arbitrary constant speed commands in the presence of unknown disturbances. The design is based on a simplified linear vehicle model which is derived from a validated nonlinear one. The designed control scheme is simulated using the validated full order nonlinear vehicle model and tested on an actual vehicle. The simulation and vehicle test results are included in this paper to show the performance of the controller. Due to the learning capability of the adaptive control scheme, changes in the vehicle dynamics do not affect the performance of the controller in any significant manner.

1 Introduction

Advanced Vehicle Control Systems (AVCS) are important parts of Intelligent Vehicle Highway Systems (IVHS). The goal of AVCS is to introduce more automatic features in vehicles by using sophisticated control systems, sensors and computers. These features may vary from the simple cruise control system currently available in vehicles, to a fully automated vehicle where the driver and passengers are not part of the

*This work is supported by Caltrans through PATH of University of California and Ford Motor Company.

control system. Partially or fully automated vehicles may be part of system architectures that include the highway. Such architectures have been shown to have strong potential for dramatically increasing the capacity of freeways[1-5] and improving the smoothness of traffic flows [5].

An important component of AVCS is the design of control systems for electronic throttle. One of the objectives of throttle control is to achieve automatic vehicle following in the longitudinal direction by following the speed response of the lead vehicle and at the same time keeping a safe intervehicle spacing [6].

In this paper we design an adaptive control scheme for throttle control that guarantees good speed tracking. This design will lay down a basis for the design of the control system for automatic vehicle following. It can also improve the cruise controller currently available in vehicles. The currently available cruise control systems are capable of locking to a particular desired speed provided that such speed exceeds 25 to 30 mph. However, there is a noticeable speed tracking error when the vehicles are going up or down hill. In contrast, our control scheme can achieve good speed tracking at all speeds and reject the effects of disturbances that may arise due to load changes, aerodynamic drag, up and down hills, etc, provided that there is sufficient engine torque to control the speed in these situations. This good performance and the capability to accept direct speed commands make the controller suitable for automatic vehicle following applications. (For example, it can be used to control the throttle of the leading vehicle in a platoon of vehicles.) The scheme is designed based on a simplified linear vehicle model which is derived from a validated nonlinear model of a vehicle. However, the learning capability of the proposed adaptive controller allows the accommodation of changes in vehicle dynamics and therefore the controller can be applied to different vehicles with little or no change.

A discrete-time version of the controller was first simulated using the validated nonlinear model and then tested on an actual vehicle in a test track. The simulation and experimental results demonstrate the effectiveness and good tracking properties of the proposed controller.

2 Longitudinal Vehicle Model

Figure 1 shows the basic diagram and inputs, outputs of a longitudinal vehicle model.

Each block in Figure 1 can be considered as a subsystem with various inputs and outputs. The output of the engine subsystem is the engine torque that is a nonlinear

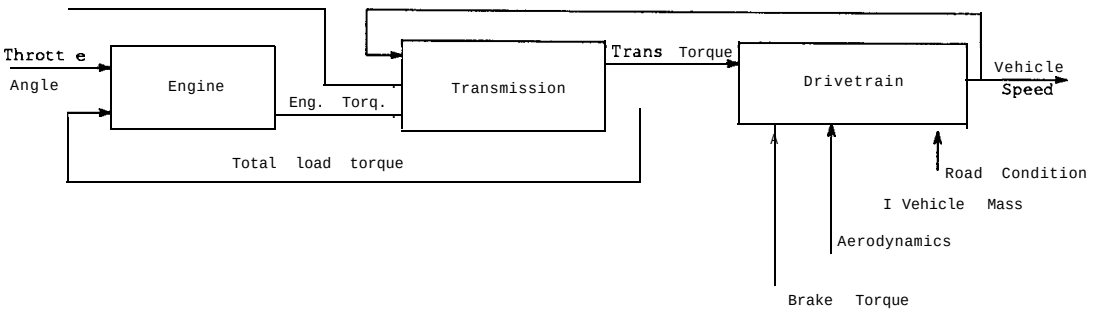

Figure 1: Vehicle Model

function of the air/fuel ratio, the exhaust gas recirculation (EGR), the cylinder total mass charge, the spark advance, the engine speed and the total load torque as well as the throttle angle. The spark advance, EGR and air-to-fuel ratio are the outputs of an internal controller (inside the engine block of Fig.1).

The transmission subsystem is responsible for transferring engine torque to the drivetrain depending on the vehicle speed and engine state. The transmission considered in Figure 1 is an automatic transmission with hydraulic torque coupling and four forward transmission gears. The gear state is a discrete nonlinear function of throttle angle, engine speed and vehicle speed.

The drivetrain subsystem receives a transmission torque and/or brake torque input and outputs vehicle speed, acceleration or deceleration. Vehicle speed and acceleration are affected by the road condition, aerodynamic drag and vehicle mass. The relationship between vehicle speed and transmission torque is also nonlinear.

For speed control, the system in Figure 1 may be considered as having two control input variables (i.e., throttle angle and brake torque) and one output (i.e., vehicle speed). In this paper we concentrate on speed control using the throttle only and therefore the brake torque is set to be zero.

The complexity of the nonlinear vehicle model described above makes it almost impossible to design a control law directly based on such a model. In our approach we employ linearization to obtain a linear model whose parameters are functions of operating points which we then use to design an adaptive controller. The linearization procedure is described as follows:

Let V_0 be the steady state vehicle speed due to a constant throttle input θ_0. Define $\bar{V} \triangleq \boldsymbol{V} - V_0$ to be the deviation of the vehicle velocity $\boldsymbol{V}$ from V_0, and $\bar{\theta} \triangleq \theta - \theta_0$

to be the deviation of throttle angle θ from θ_0. Using the validated nonlinear vehicle model we find that, for any fixed gear state, the linearized model that relates $\bar{V}, \bar{\theta}$ over a wide range of speed V_0 (from 0 $\rightarrow$ 80 mph) has the form

$$\frac{\bar{V}}{\bar{\theta}} = \frac{b_0}{s^3 + a_2 s^2 + a_1 s + a_0} = \frac{b_0}{(s+p_1)(s+p_2)(s+p_3)} \tag{1}$$

where the coefficients b_0, a_0, al, a_2 are functions of the operating point V_0 or (θ_0, V_0), i.e., b_0, a; have different values for different θ_0, V_0.

For all operating points considered, however, we found that all poles have **negative** real parts and p_1 is real. Furthermore, $Re(p_2), Re(p_3) >> p_1$ and Cl $< p_1 \leq$ 0.2. A measure of how far apart $Re(p_2), Re(p_3)$ are from p_1 can be given by the value of a variable λ defined as

$$\lambda = \inf_{\theta_0 \in \Theta} \min \left[\left| \frac{Re(p_i)}{p_1} \right|, i = 2, 3 \right] \tag{2}$$

where Θ is the full change range of θ. Our results show that $\lambda > 20$ which indicates that $-p_1$ is the dominant pole and that the fast modes associated with p_2, p_3 can be neglected, leading to the simpler model of

$$\frac{\bar{V}}{\bar{\theta}} = \frac{b}{s + a} \tag{3}$$

where a, *b* vary with V_0. The effects of the fast mode terms and uncertainties neglected in the linearization procedure may be modeled as a disturbance term d, leading to the model

$$\dot{\bar{V}} = -a\bar{V} + b\bar{\theta} + d \tag{4}$$

or equivalently,

$$\dot{V} = -a(V - V_0) + b\bar{\theta} + d. \tag{5}$$

In our experiments a changes from 0.2 to 0.03 when V_0 changes from 0 to 80 mph. However, a, *b* may change due to other effects such as changes in aerodynamic drag and load, deterioration of certain mechanical functions, etc. For these reasons we take a, *b*, d to be unknown and propose a control scheme that does not depend on the values of a, *b*, *d*. The scheme is an adaptive controller and is presented in the next sections.

3 Continuous-time Adaptive Cruise Control

Let V_d be the desired speed that we like to track. The objective of the adaptive control design is to make the vehicle speed follow the response of the reference model

$$\dot{V}_m = -a_m V_m + a_m V_d \tag{6}$$

where a, > 0 is chosen based on the requirement of system response speed, riding quality etc. The reference model is used to smooth the trajectory of the desired velocity V_d. It is obvious that, for constant V_d, V_m equals V_d at steady state. Thus, tracking V_m is similar to tracking V_d but in a smooth way.

To achieve the control objective we propose the adaptive control design shown in Figure 2.

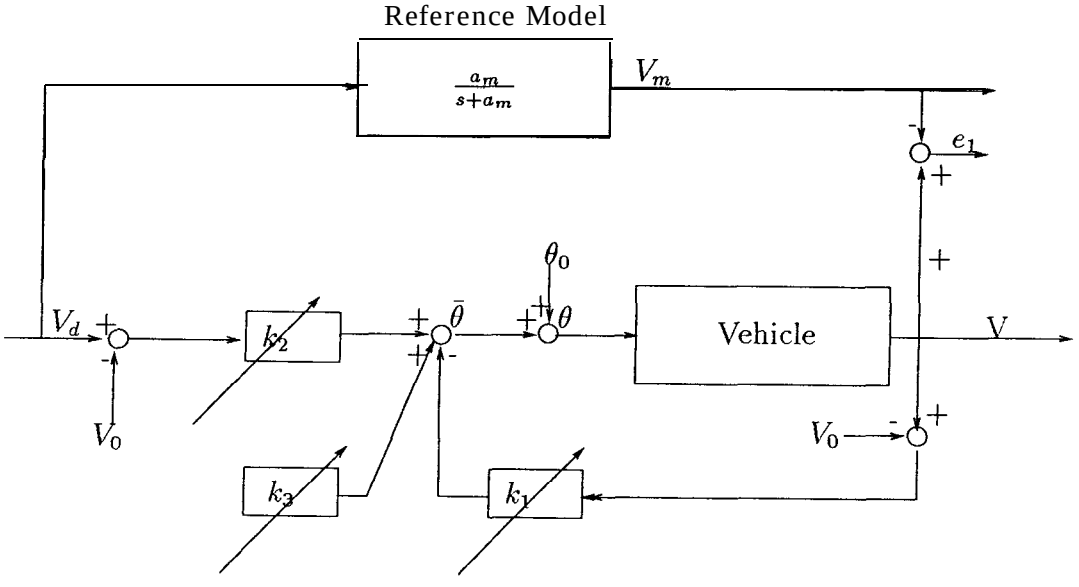

Figure 2: Adaptive Control Scheme

It follows from Figure 2 that

$$\bar{\theta} = -k_1 \bar{V} + k_2(V_d - V_0) + k_3 \tag{7}$$

where k_1, k_2, k_3 are time varying gains to be generated by an adaptive law. Substituting equation (7) into equation (5), we obtain that

$$\dot{V} = -(a + bk_1)(V - V_0) + bk_2(V_d - V_0) + bk_3 + d. \tag{8}$$

If a, b, d were constant and known, then we could choose $k_1 = k_1^*, k_2 = k_2^*, k_3 = k_3^*$ where k_1^*, k_2^*, k_3^* satisfy

$$\begin{aligned} bk_1^* &= a_{,,,} - a \\ bk_2^* &= a_{,} \\ bkj &= -d \end{aligned} \tag{9}$$

which would make equation (8) to be the same as equation (6). Since a, b, and d are unknown, k_i^* cannot be calculated from equation (9). Instead we develop an adaptive law for generating k_i, the estimate of $k_i^*, i = 1, 2, 3$, on-line as follows:

Let $e_1 \triangleq V - V_m$ be the tracking error. Then from equations (8), (6) and (9), we have that

$$\dot{e}_1 = -a_m e_1 + b\left[-\tilde{k}_1 \bar{V} + \tilde{k}_2(V_d - V_0) + \tilde{k}_3\right] \tag{10}$$

where $\tilde{k}_i = k_i - k_i^*$, $i = 1, 2, 3$, are the parameter errors. Equation (10) may be also written as

$$e_1 = \frac{b}{s + a_{,}}\left[-\tilde{k}_1 \bar{V} + \tilde{k}_2(V_d - V_0) + \tilde{k}_3\right]. \tag{11}$$

We define the new error signal

$$\varepsilon = e_1 - \frac{1}{s + a_{,}} \varepsilon e_1^2 \tag{12}$$

which together with (11) implies that

$$\dot{\varepsilon} = -a_m \varepsilon - b\tilde{k}_1 \bar{V} + b\tilde{k}_2(V_d - V_0) + b\tilde{k}_3 - \varepsilon e_1^2. \tag{13}$$

The signal ε is the so called normalized estimation error defined in [7]. From this definition we see that at steady state, ε is roughly equal to $a_m e_1/(a_m + e_1^2)$. Thus if $e_1 \gg 1$, then $\varepsilon \ll e_1$ and if $e_1 << 1$ then $\varepsilon \approx e_1$. As seen below, we will use ε instead of e_1 to update k_1, k_2, k_3. The reasons are that ε is a normalized version of e_1 and therefore with ε, the adjustment of $k_i, i = 1, 2, 3$, is slow relative to the possible rapid changes in e_1. This slow speed of adaptation helps robustness by keeping the bandwidth of the controller in the low frequency range. The adaptive law is derived by using the Lyapunov-like function

$$V_\ell = \frac{\varepsilon^2}{2} + b\frac{\tilde{k}_1^2}{2\gamma_1} + b\frac{\tilde{k}_2^2}{2\gamma_2} + b\frac{\tilde{k}_3^2}{2\gamma_3} \tag{14}$$

where $\gamma_i > 0$ and b, even though unknown, is known to be always positive at all operating points. The time derivative of V_ℓ along the solution of (13) is

$$\dot{V}_\ell = -a_m \varepsilon^2 - \varepsilon^2 e_1^2 - \varepsilon b\tilde{k}_1 \bar{V} + \varepsilon b\tilde{k}_2(V_d - V_0) + \varepsilon b\tilde{k}_3 + \sum_{i=1}^{3} b\frac{\tilde{k}_i \dot{\tilde{k}}_i}{\gamma_i}. \tag{15}$$

Choosing

$$\begin{aligned} \dot{k}_1 &= \gamma_1 \varepsilon \bar{V} \\ \dot{k}_2 &= -\gamma_2 \varepsilon (V_d - V_0) \\ \dot{k}_3 &= -\gamma_3 \varepsilon \end{aligned} \tag{16}$$

we have that

$$\dot{V}_\ell = - a_m \varepsilon^2 - \varepsilon^2 e_1^2 \tag{17}$$

which together with additional stability arguments given in [7] guarantees that $\varepsilon, e_1 \to 0$ as $t \to$ co and k_1, k_2, k_3 are bounded. For robustness the adaptive laws for $k_i, i = 1,2,3$, in (16) can be modified to

$$\dot{k}_i = \begin{cases} 0 & \text{if } k_i \geq k_{u_i} \text{ and } \varepsilon X_i > 0 \\ 0 & \text{if } k_i \leq k_{\ell_i} \text{ and } \varepsilon X_i < 0 \\ \gamma_i X_i \varepsilon & \text{otherwise} \end{cases} \tag{18}$$

where k_{u_i}, k_{ℓ_i} are respectively the upper bound and lower bound for k_i and $X_1 = \bar{V}, X_2 = -(V_d - V_0)$ and X_3 = -1. The modified adaptive law (18) guarantees that $k_{\ell_i} \leq k_i(t) \leq k_{u_i} \quad \forall t \neq 0$ provided $k_i(0)$ satisfies $k_{\ell_i} \leq k_i(0) \leq k_{u_i}$. By constraining the gains k_i within certain bounds we avoid the generation of high gain feedback that may cause instability or deterioration of performance due to excessive excitation of the unmodeled dynamics. As shown in [7], the stability properties of (16) are improved with this modification.

The inputs V_0, θ_0 shown in Figure 2 depend on the operating point and are related to each other. We can do a series of experiments to find the one-to-one correspondence between steady state vehicle speed and the throttle angle. From this one-to-one correspondence, we can get the function

$$\theta_0 = f^{-1}(V_0). \tag{19}$$

Since V_d is the desired speed and V_0 is the operating point we like to reach, it makes sense to assume that $V_d = V_0$. With this assumption we have that $\dot{k}_2 = 0$,

$$\theta_0 = \theta_d = f^{-1}(V_d),$$

equation (7) is simplified to

$$\bar{\theta} = -k_1(V - V_d) + k_3, \tag{20}$$

the throttle angle command becomes

$$\theta = f^{-1}(V_d) - k_1(V - V_d) + k_3, \tag{21}$$

and the adaptive laws are replaced with

$$\dot{k}_i = \begin{cases} 0 & \text{if } k_i \geq k_{u_i} \text{ and } \varepsilon X_i > 0 \\ 0 & \text{if } k_i \leq k_{\ell_i} \text{ and } \varepsilon X_i < 0 \\ \gamma_i X_i \varepsilon & \text{otherwise} \end{cases} \tag{22}$$

where i = $1, 3, X_1 = V - V_d, X_3 = 1$.

The adaptive controller described above is a PI controller with adjustable proportional gain. This proportional gain may cause a large throttle angle change and hence large jerk when $|V - V_d|$ is large. In order to avoid excessive throttle inputs, we use sat(V $- V_d$) instead of $V - V_d$ in equations (20) and (21) where

$$\text{sat}(V - V_d) = \begin{cases} \text{A} & \text{if } V - V_d > \Delta \\ V - V_d & \text{if } |V - V_d| \leq \text{ A} \\ \text{- A} & \text{if } V - V_d < -\Delta \end{cases}$$

where A is an allowable upper bound for $|V - V_d|$. To further smooth the throttle command and avoid the presence of high frequency components in θ, we filter the speed command V_c with a low pass filter $\frac{c}{s+c}$ whose output is the desired speed V_d.

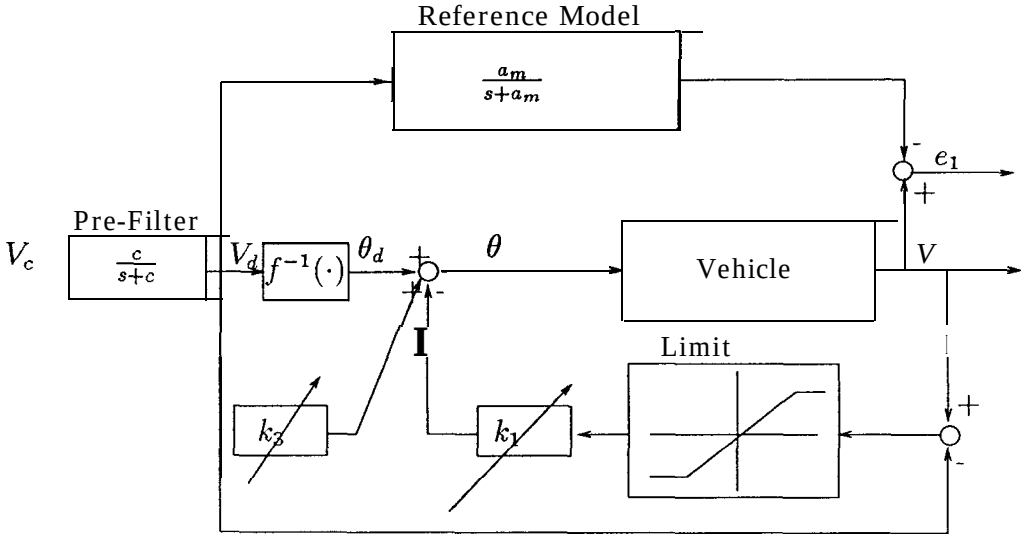

Figure 3: Augmented Adaptive Control Scheme

With these modifications, the new adaptive control scheme is shown in Figure 3 and is summarized below:

$$
\begin{aligned}
\theta &= f^{-1}(V_d) - k_1 \,\mathrm{sat}(V - V_d) + k_3 \\
\dot{V}_d &= -cV_d + cV_c \\
\dot{V}_m &= -a_m V_m + a_m V_d \\
\dot{k}_i &= \begin{cases} 0 & \text{if } k_i \geq k_{u_i} \text{ and } \varepsilon X_i > 0 \\ 0 & \text{if } k_i \leq k_{\ell_i} \text{ and } \varepsilon X_i < 0 \\ \gamma_i \varepsilon X_i & \text{otherwise} \end{cases} \\
\dot{\varepsilon} &= -(a, + e_1^2)\varepsilon + \dot{e}_1 + a_m e_1 \\
e_1 &= v - v,
\end{aligned}
$$

where i $=1,3$, $X_1 = V - V_d$, X_3 = -1. We refer to the adaptive controller shown in Figure 3 as the augmented adaptive controller.

4 Discrete-time Adaptive Cruise Control

While the continuous-time controller developed in section 3 is useful for analysis when applied to the continuous-time physical model, its implementation on a digital computer requires a discrete-time version of the controller. The purpose of this section is to develop such a discrete-time controller.

Due to the high sampling rate relative to the frequencies and time constants present in the vehicle speed response we can discretize each dynamic equation separately.

The dynamic equations of the form

$$\dot{x} = \text{--ax + bu.}$$

are discretized based on the rule of bilinear transformation, i.e., substituting $\frac{2(z-1)}{T(z+1)}$ for s, where z is the Z-transform or forward operator and T is the sampling period. According to this rule, we have that

$$V_d(t+T) = \alpha_d(T)V_d(t) + \beta_d(T)[V_c(t+T) + V_c(t)]$$

and

$$V_m(t+T) = \alpha_m(T)V_m(t) + \beta_m(T)[V_d(t+T) + V_d(t)]$$

where

$$\alpha_d(T) = \frac{2 - cT}{2 + cT}, \qquad \beta_d(T) = \frac{cT}{2 + cT},$$
$$\alpha_m(T) = \frac{2 - a_m T}{2 + a_m T}, \qquad \beta_m(T) = \frac{a_m T}{2 + a_m T}.$$

The pure limited integrators in the dynamic equations for k_1 and k_3 are discretized by replacing the integrator l/s with the block $Tz/(z-1)$ and by including a saturation block as follows:

$$k_i(t + T) = \begin{cases} k_{u_i} & \text{if } \gamma_i X_i(t+T)\varepsilon(t + T)T + k_i(t) > k_{u_i} \\ k_{l_i} & \text{if } \gamma_i X_i(t + T)\varepsilon(t + T)T + k;(t) < k_{l_i} \\ \gamma_i X_i(t + T)\varepsilon(t + T)T + k;(t) & \text{otherwise} \end{cases}$$

where i = $1, 3, X_1 = V - V_d, X_3 =$ -1.

At last we discretize the dynamic equation for ε. Since this equation is nonlinear and stiff in some sense when e_1 is large, we use the backward Euler method to discretize it. With this method we approximate $\dot{x}(t + T)$ as

$$\dot{x}(t + T) \approx \frac{x(t + T) - x(t)}{T}.$$

Using the above approximation we obtain

$$[\varepsilon(t+T) - \varepsilon(t)]/T = -[a_m + e_1^2(t + T)]\varepsilon(t+T) + [e_1(t+ T) - e_1(t)]/T + a_m e_1(t + T),$$

which implies that

$$\varepsilon(t + T) = \frac{\varepsilon(t) + (1 + a_m T)e_1(t + T) - e_1(t)}{1 + [a, + e_1^2(t+T)]T}.$$

The reason for using the backward Euler method is to avoid instability due to large $e_1^2(t+ T)$ that may occur when the bilinear transform method is used.

The discrete-time adaptive controller is shown in Figure 4 and is summarized below:

$$\theta = f^{-1}(V_d) - k_1 \text{sat}(V - V_d) + k_3$$
$$V_d(t + T) = \alpha_d V_d(t) + \beta_d(V_c(t + T) + V_c(t))$$
$$V_m(t+ T) = \alpha_m V_d(t) + \beta_m(V_c(t + T) + K(t))$$

$$
k_i(t+T) = \begin{cases} k_{u_i} & \text{if } \gamma_i X_i(t+T)\varepsilon(t+T)T + k_i(t) > k_{u_i} \\ k_{l_i} & \text{if } \gamma_i X_i(t+T)\varepsilon(t+T)T + k_i(t) < k_{l_i} \\ \gamma_i X_i(t+T)\varepsilon(t+T)T + k_i(t) & \text{otherwise} \end{cases}
$$

$$
\varepsilon(t+T) = \frac{\varepsilon(t) + (1 + a_m T)e_1(t+T) - e_1(t)}{1 + (a, + e_1^2(t+T))T} \qquad (23)
$$

$$
e_1 = V - V_m
$$

where $i = 1, 3$, and X_i, sat(.) are defined as before.

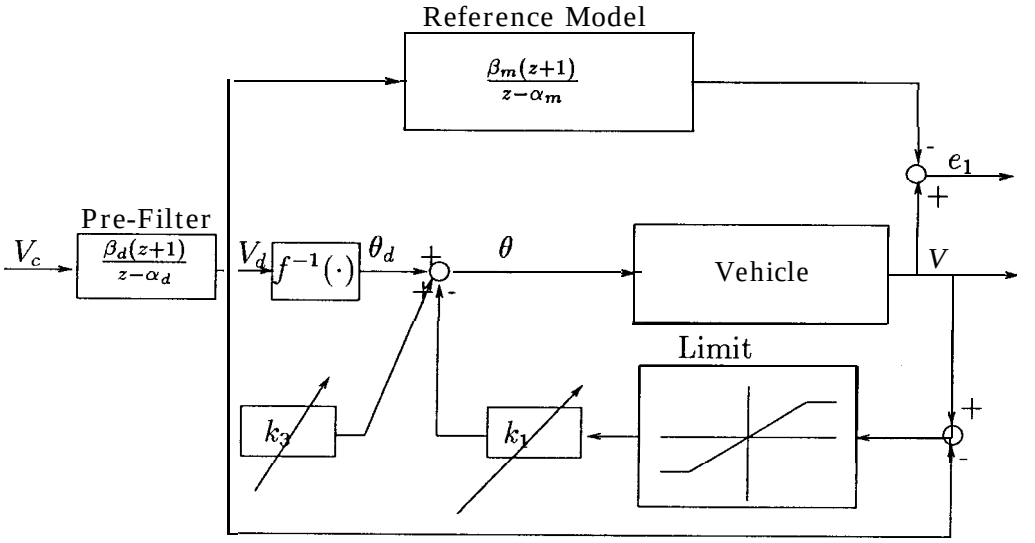

Figure 4: Discrete Time Adaptive Control Scheme

5 Simulation and Experimental Results

The adaptive throttle controller designed in Section 4, which is the discrete-time version of the augmented adaptive controller shown in Figure 3, was applied to the validated full order nonlinear vehicle model for simulation. In the simulations, the following constants and design parameters were chosen:

$$
\gamma_1 = \gamma_3 = 2, \quad a, = c = 1, \quad k_{u_1} = 8, \quad k_{\ell_1} = 2
$$

$k_1(0)$ = 2.5, $k_3(0)$ = 0, K_{u_3} = 40, K_{l_3} = -40, A = $4(mph)$.

In addition, because of the hardware limitations of the throttle actuator, we added to the throttle angle output a derivative limit block which limits the rate of change of the throttle angle θ to be in the range of $\pm 100\,\text{degree/sec}$ and another saturation element that limits the throttle angle θ to be in the range of $3 \leq \theta \leq 85$ degree.

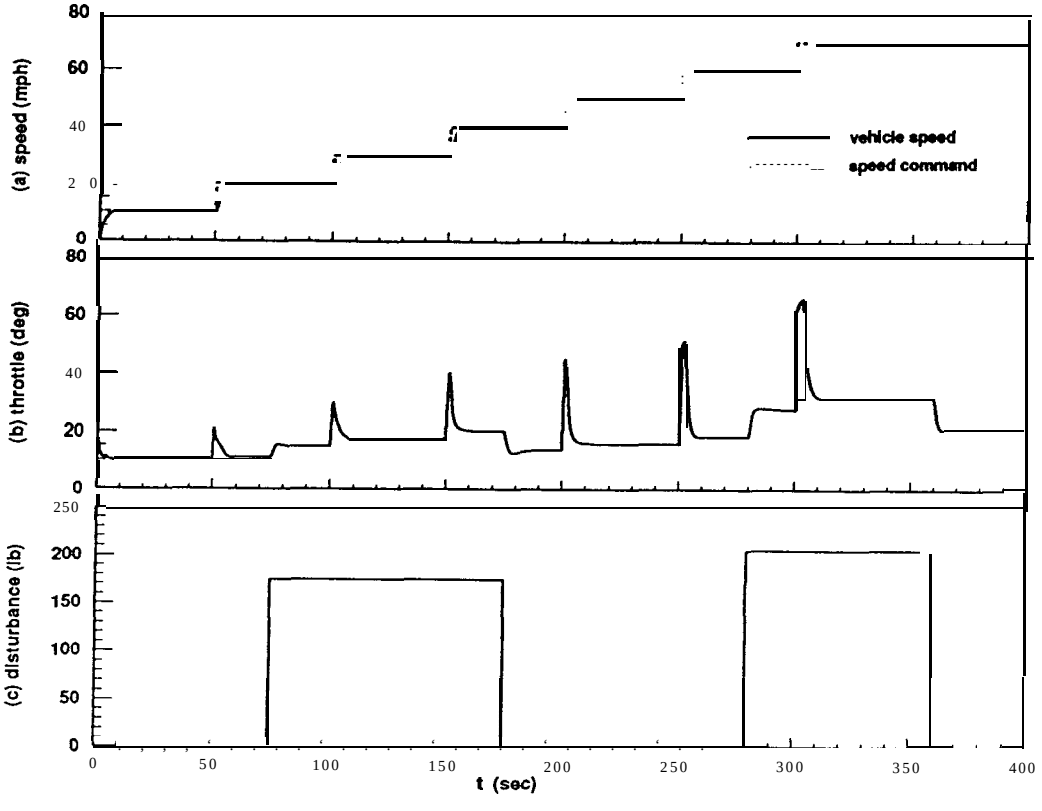

Figure 5: Simulation results with staircase speed command

Figures 5(a), 5(b) show the vehicle speed response and throttle command response to a staircase speed command respectively in the presence of the load disturbance shown in Figure 5(c). This disturbance is equivalent to the one encountered in an up hill situation with a slope of 3 to 4 percent. It is clear that the vehicle speed follows the desired one quite accurately without any oscillations and the effect of the disturbance is rejected fairly fast.

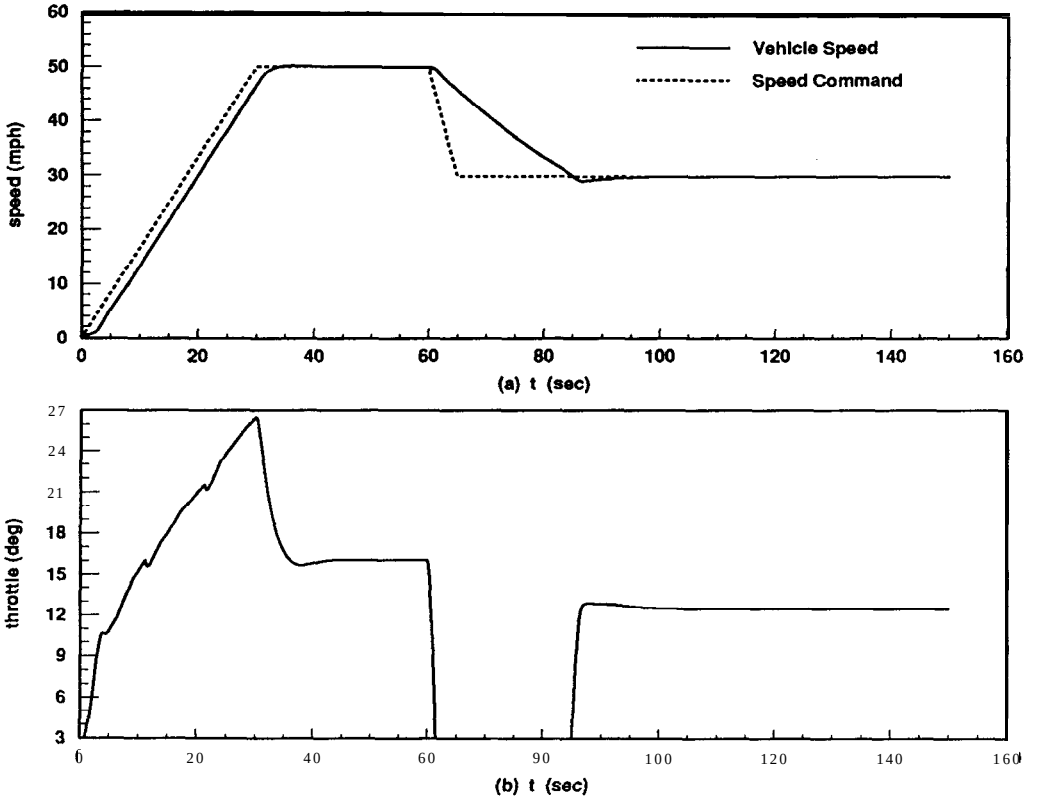

Figure 6: Simulation results with ramp speed command

Figures 6(a) and 6(b) show the vehicle speed and throttle response to a ramp speed command that involves acceleration and deceleration. It is seen that the tracking is quite accurate when the desired speed is increasing or is constant as shown in Figure 6(a). When the desired speed is decreasing the control law is no longer as effective without the use of brakes. However, it does what a good driver will do when he wants to slow down without the use of brakes. He switches to the lowest throttle input until the speed is sufficiently reduced and then he increases the throttle to a certain degree in order to maintain the desired speed. This is exactly the type of response achieved by the adaptive controller as shown in Figure 6(b).

The same controller was also tested on an actual vehicle in a test track. The test track was a fairly rough road and the number of passengers was changed from one test to another in order to check the effect of load disturbance. One of these test results is described as follows:

Figure 7(a) shows the desired speed command and the vehicle speed. Initially, the

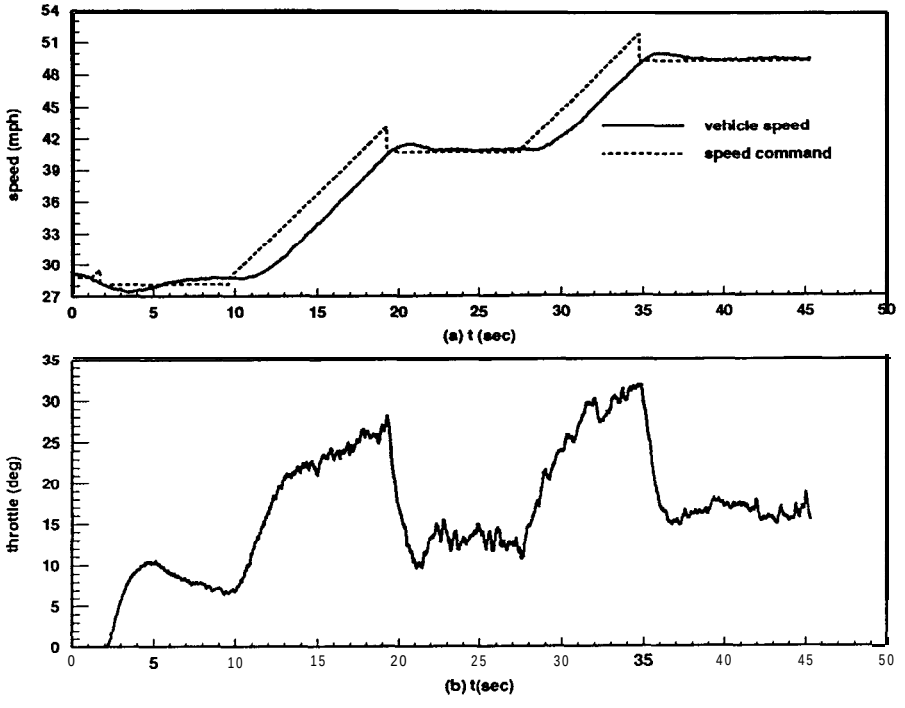

Figure 7: Experimental results with adaptive throttle control

vehicle is at a speed of about 29 mph when the adaptive controller was turned on. From $t \approx 0$ to $t \approx 10$ seconds the vehicle's speed was maintained at the desired speed ≈ 28 mph. From $t \approx 10$ to $t \approx 20$ seconds the desired speed was increased to 40 mph. During this time interval, the vehicle speed was tracking the desired speed within 2 mph of error. From $t \approx 20$ to $t \approx 28$ seconds, the desired speed was maintained at about 40 mph. So did the vehicle speed and there was no steady state error. From $t \approx 28$ to $t \approx 45$ seconds, the desired speed was increased to 48 mph first and then kept constant. During this time interval, the vehicle speed tracking was also quite accurate. Figure 7(b) shows the corresponding throttle command.

6 Conclusion

In this paper we designed an adaptive throttle controller for speed tracking. The controller was designed based on a simplified linear model derived from a validated nonlinear model. Simulations and vehicle tests show that this controller can achieve good

speed tracking for any constant speed command in the presence of load disturbances. Moreover, because of its learning capability, the control scheme can accommodate possible changes in vehicle dynamics due to different vehicles, aging, and wear etc.

Acknowledgments

We would like to thank the following Ford researchers: Dr. Mike Shulman, Dr. Steve Eckert, Dr. Durk Wuh, and Mr. David Clemons, Mr. Melvin Palmer, Mr. Tom Pilutti, and Mr. Richard Ames for their expert explanations and comments regarding vehicle dynamics and control and for their help in performing the experiments.

References

[1]. S. E. Shladover, Longitudinal Control of Automotive Vehicles in Close-Formation Platoons, *ASME Journal on Dynamic Systems, Measurement and Control,* vol.113, pp. 231-241, 1991.

[2]. S. E. Shladover, C. A. Desoer, J. K. Hedrick, M. Tomizuka, J. Walrand, W. B. Zhang, D. McMahon, H. Peng, S. Sheikholeslam, and N. McKeown, Automatic Vehicle Control Developments in the PATH Program, *IEEE Trans. on Vehicular Technology,* vol. 40, pp. 114-130, 1991.

[3]. S. Sheikholeslam and C. A. Desoer, A System Level Study of the Longitudinal Control of a Platoon of Vehicles, *ASME Journal on Dynamic Systems, Measurement, and Control,* 1991.

[4]. P. Varaiya, Smart Cars on Smart Roads: Problems of Control, PATH Technical Memorandum, 91-S, December 1991.

[5]. C. C. Chien and P. Ioannou, Automatic Vehicle Following, *Proc. American Control* Conference, Chicago, Il., June 1992.

[6]. J. K. Hedrick, D. McMahon, V. Narendran, and D. Swaroop, Longitudinal Vehicle Controller Design for IVHS System, *Proc. American Control Conference,* vol.3, pp. 3107-3112, June 1991.

[7]. P. Ioannou and A. Datta, Robust Adaptive Control: A Unified Approach, *Proc.* of *the IEEE*, vo1.79, pp. 1736-1769, December 1991.